A segmented, graph-optimized segmentation that positions and plots at the same time

Qinyu Niu[a], Yong Zhao[*], Meifan Li[b]

Xi'an University of Science and Technology, Xi'an, China

*Corresponding Author Email: 931643857@qq.com, [a]417594863@qq.com, [b]1224162935@qq.com

Abstract. Aiming at the process of simultaneous positioning and mapping (SLAM) of traditional lidar, the lidar scanning frame only matches the current submap, and with the continuous increase of submaps, the error continues to accumulate, resulting in problems such as the global map cannot be closed loop, and the global map distortion is proposed. According to the IMU angular velocity data, when the IMU angular displacement changes greatly, the system will reduce the trust value of the IMU data at this time according to the dynamic weight distribution coefficient, and use this moment as the starting point of the segment, reconstruct the local subgraph, and add loopback constraints to it. The next frame of radar data is used as the initial pose to construct the local submap again, cycle through it in turn, and finally optimize each local submap to build a complete map by means of global map optimization. After experimental verification, the algorithm can effectively improve the distortion of the global map caused by the excessive rotation angle, which is of practical significance.

Keywords: graphoptimiation, loopdetection, SLAM.

1. Introduction

In recent years, with the vigorous development of the robot industry, from industrial AGV and storage industry to floor sweeping robot, the progress of simultaneous localization and mapping (SLAM) [1] is the prerequisite for its progress, and the progress of slam technology directly affects the development of the industry. Slam technology refers to that the robot carries a sensor and independently constructs and corrects the environmental map when the environmental information is unknown. Smith, self and Cheeseman put forward the concept of slam in 1986. In future research, slam has always been a prerequisite for the development and progress of robots.

With the progress of society, slam technology is also steadily upgrading. Slam sensors mainly include three forms: vision based sensor [2-3], lidar based sensor [4-5] and ultrasonic radar. When a mobile robot constructs an incremental [6] environment map in an unknown search area, the error accumulation of sensor data [7] will be caused due to the algorithm, resulting in map drift and other problems in the environment map constructed by the robot. Therefore, the concept of Closed-loop Detection [8] is proposed. Closed loop detection is generally carried out in the process of building local map and global optimization. Find the appropriate loop and add constraints to the graph optimization [9-10]. However, when the robot runs in a large area for a long time in a large scene, the number of loops added will be very large, which will lead to the back-end of graph optimization can not perfectly coordinate each loop constraint and build an error free environment map. When the loop back constraint is calculated at the front end, due to the limitation of system processing speed, new data will accumulate in the process pool. The introduction of delay makes it difficult to deal with and update the map in time. Olson determines whether the observed scene overlaps by calculating the Mahalanobis distance [11] between poses. However, because the lidar scanning frame is only matched with the current local map, and the map optimization is only carried out at the back end, with the continuous increase of sub maps, the error is bound to accumulate and lead to the distortion of the global map. Moreover, the cumulative error of angle has an irreparable impact on the construction of global map, which will lead to the situation that the head and tail cannot be closed-loop.

This paper proposes a segmented loop detection slam scheme based on graph optimization. According to the IMU angular velocity data, when the IMU angular displacement changes greatly,

the system will reduce the IMU data trust value according to the dynamic weight distribution coefficient, and take this time as the segmentation starting point to reconstruct the local sub graph to ensure the accuracy of the local map. Take the radar data of the next frame as the initial pose, construct the local subgraph again, cycle in turn, and finally globally optimize each local subgraph by means of global graph optimization to construct a complete map.

2. IMU and radar model

2.1. IMU pose estimation

IMU is a combination of acceleration sensor and angular velocity sensor, which can be used to measure the three-axis attitude angle and acceleration of the object. After integrating the data, the angular displacement, velocity and mileage information can be obtained. At time n, the position and attitude of the car in the world coordinate system is$(x_n,\ y_n,\ \theta_n)^T, (\delta_d\ , \delta_\theta)$ Represents the mileage and angular displacement of AGV at time n + 1. The position and attitude of the trolley at time n + 1 is expressed in the world coordinate system as:

$$\xi_n \sim \begin{pmatrix} \cos\ \theta_n & -\sin\ \theta_n & x_n \\ \sin\ \theta_n & \cos\ \theta_n & y_n \\ 0 & 0 & 1 \end{pmatrix} \tag{1}$$

The angular displacement and mileage of the trolley from n to N + 1 are very small. The angular displacement is δ_θ,and the mileage is δ_d,so the position and attitude of the trolley at n + 1 are obtained ξ_{n+1}:

$$\begin{aligned} \xi_{n+1} &= \begin{pmatrix} \cos\ \theta_n & -\sin\ \theta_n & x_n \\ \sin\ \theta_n & \cos\ \theta_n & y_n \\ 0 & 0 & 1 \end{pmatrix} \begin{pmatrix} \cos\ \delta_\theta & -\sin\ \delta_\theta & 0 \\ \sin\ \delta_\theta & \cos\ \delta_\theta & 0 \\ 0 & 0 & 1 \end{pmatrix} \begin{pmatrix} 1 & 0 & \delta_d \\ 0 & 1 & 0 \\ 0 & 0 & 1 \end{pmatrix} \\ &= \begin{pmatrix} \cos(\theta_n + \delta_\theta) & -\sin(\theta_n + \delta_\theta) & x_n + \delta_d \cos(\theta_n + \delta_\theta) \\ \sin(\theta_n + \delta_\theta) & \cos(\theta_n + \delta_\theta) & y_n + \delta_d \sin(\theta_n + \delta_\theta) \\ 0 & 0 & 1 \end{pmatrix} \end{aligned} \tag{2}$$

It can be expressed by three-dimensional vector as:

$$\xi_{n+1} = \begin{pmatrix} x_n + (\delta_d + e_d)\cos\ (\theta_n + \delta_\theta + e_\theta) \\ y_n + (\delta_d + e_d)\sin\ (\theta_n + \delta_\theta + e_\theta) \\ \theta_n + \delta_\theta + e_\theta \end{pmatrix} \tag{3}$$

Generally, IMU noise can be modeled as the variance of a zero mean Gaussian distribution:

$$E_{IMU} = \begin{pmatrix} \sigma_d^2 & 0 \\ 0 & \sigma_\theta^2 \end{pmatrix} \tag{4}$$

amongσ_θ^2 represents the gyro noise parameter,σ_d^2 represents the noise parameter of accelerometer.

2.2. Lidar model

Note that the center point of the trolley is O, and the lidar is installed at the distance L from the center point directly above the trolley. For the measuring point A, it is expressed as in polar coordinate system relative to the lidar $(\rho_{laser}\ \varphi_{laser})^T$. Then, the position and attitude of measuring point A in the world coordinate system can be expressed by three-dimensional vector:

$$\xi_A = \begin{pmatrix} x_n + \mathrm{L}\cos\theta_r + \rho_{\mathrm{laser}}\ \cos(\theta_r + \varphi_{\mathrm{laser}}) \\ y_n + \mathrm{L}\sin\theta_r + \rho_{\mathrm{laser}}\ \sin(\theta_r + \varphi_{\mathrm{laser}}) \\ \theta_r + \varphi_{\mathrm{laser}} \end{pmatrix} \tag{5}$$

Record the lidar measurement noise as e_ρ and e_φ,Add the measurement noise to the above equation to obtain the pose of measurement point A, which can be expressed as:

$$E_{laser} = \begin{pmatrix} x_n + L\cos\ \theta_n + (\rho_{\text{laser}} + e_\rho)\cos(\theta_r + \theta_{\text{laser}} + e_\varphi) \\ y_n + L\sin\ \theta_n + (\rho_{\text{laser}} + e_\rho)\sin(\theta_r + \theta_{\text{laser}} + e_\varphi) \\ \theta_r + \theta_{\text{laser}} + e_\varphi \end{pmatrix} \tag{6}$$

The measurement noise can be modeled as:

$$E_{laser} = \begin{pmatrix} \sigma_\rho^2 & 0 \\ 0 & \sigma_\varphi^2 \end{pmatrix} \tag{7}$$

$\sigma_\rho^2, \sigma_\varphi^2$ represents the range and angle noise parameters of lidar respectively.

3. Segmented loop detection

3.1.Segmented loop detection method

Due to the inevitable large-scale angular displacement movement of the trolley in the process of traveling, this movement leads to the instability of loop detection, and then affects the accuracy of global slam. The segmented loop detection method is to judge the fluctuation amplitude of IMU angular displacement according to the variance of IMU angular velocity data. When the transformation amplitude of angular displacement is large, the system will reduce the trust value of IMU data at this time according to the dynamic weight distribution coefficient, and take this time as the segmented starting point to reconstruct the local subgraph. The flow chart is shown in the “Fig.1” below:

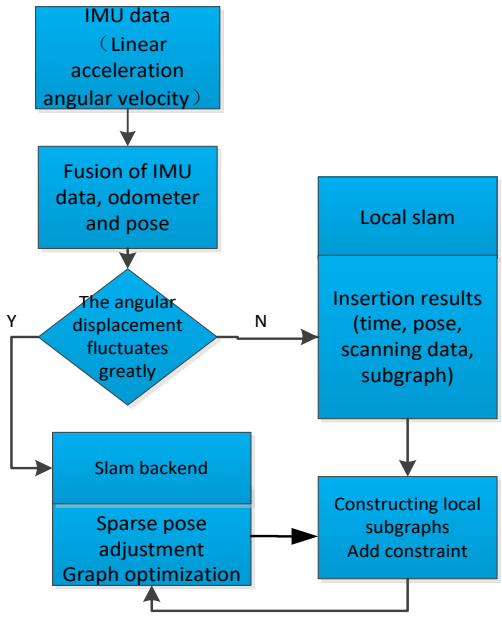

Fig.1 Optimization flow chart

Each time the local subgraph is constructed, the next frame of radar data scan is used as the local first frame data to reconstruct the graph. When all the local subgraphs of the car are built to the global slam, the local subgraphs are added to the global slam. In the process of optimization, the large global map is transformed into several small local subgraphs, and constraints are added to provide conditions for subsequent global graph optimization.

3.2.Calculation of dynamic weight distribution coefficient

When there is a large-scale disturbance in IMU data, the larger the variance will be, the more inaccurate the estimation result will be, and the smaller the weight coefficient allocated when adjusting the weight. According to the weight coefficient formula:

$$P = \left(\frac{E_{IMU}}{E_{IMU}+E_{laser}}\right)\xi_A + \left(1 - \frac{E_{IMU}}{E_{IMU}+E_{laser}}\right)\xi_{n+1} \tag{8}$$

When E_{IMU}=0, IMU has no error,It can be calculated from the above formula$P = \xi_{n+1}$,That is, fully trust IMU pose estimation. When the IMU data fluctuates greatly,When the IMU increases,the trust value of the system for IMU data decreases, so that the purpose of dynamically adjusting the weight of IMU can be achieved.

3.3.Constraint construction

Because the segmented loop back detection divides the local subgraph, we need to add constraints to the last two local subgraphs to facilitate the processing of global constraints at the back end of slam.

Assuming that during segmentation, it corresponds to the i and j nodes of the n local subgraph, then the constraint between the two nodes is represented by the error.

$$E_{laser} = e_{ij} = \bar{z}_{ij} - z_{ij} \tag{9}$$

z_{ij} is the relative pose transformation relationship between the *i* and *j* nodes established by the prediction relationship of IMU;$\bar{z}_{ij}$ is the relative pose transformation between the *i* and *j* nodes established by the lidar measurement data; Equation (3) and (6)can be brought into:

$$e_{ij}=E_{laser}\xi_{n+1}=\begin{pmatrix} x_n + L\cos\ \theta_n + \left(\rho_{\text{laser}} + e_\rho\right)\cos\left(\theta_r + \theta_{\text{laser}} + e_\varphi\right) \\ y_n + L\sin\ \theta_n + \left(\rho_{\text{laser}} + e_\rho\right)\sin\left(\theta_r + \theta_{\text{laser}} + e_\varphi\right) \\ \theta_r + \theta_{\text{laser}} + e_\varphi \end{pmatrix}$$
$$-\begin{pmatrix} x_n + (\delta_d + e_d)\cos(\theta_n + \delta_\theta + e_\theta) \\ y_n + (\delta_d + e_d)\sin(\theta_n + \delta_\theta + e_\theta) \\ \theta_n + \delta_\theta + e_\theta \end{pmatrix} \tag{10}$$

The function of loopback is to clarify the cumulative error of the system. The task of optimization is to distribute the accumulated error among all nodes to minimize the overall error, so we add the constraints constructed for local subgraphs to the back-end global optimization.

4. Global optimization

The back-end of pose graph optimization is based on the constraints of the nodes constructed by the front-end and the edges between nodes. The essence of pose graph optimization is an optimization problem, so it can be transformed into a nonlinear least squares problem to solve the optimal solution, so as to minimize the error between the pose and constraints of all nodes.

First, we put all the nodes together and record them as vectors **x**

$$\mathbf{x} = \left[\text{pose}_1,\ \text{pose}_{\ i}, \ldots,\ \text{pose}_{\ N_s}, \text{pose}_1, \text{pose}_j, \ldots,\ \text{pose}_{\ N_n}\right]^T \tag{11}$$

N_s represents the number of local subgraphs,N_n represents the number of nodes.

Take the error term between the i local subgraph and the j,node as the k of all error terms, then the overall error function between all nodes is:

$$e_k(\mathbf{x}) \triangleq e_{ij}(\mathbf{x}) = e_{ij} \tag{12}$$

Due to the $e_k(\mathbf{x})$ is a vector rather than a scalar, so the second norm of the vector is taken. At the same time, considering the weight of different elements, the weight can be reflected in the information matrix. Therefore, the size of the overall error function can be expressed as:

$$F(\xi) = e_k^T(\mathbf{x})\Omega_k e_k(\mathbf{x}) \tag{13}$$

Ω_k represents the information matrix of Gaussian distribution and is the inverse of covariance matrix.

Finally, all nodes will be optimized by using pose constraints, and the optimal pose of all nodes in the pose graph will be found to minimize the overall error function:

$$\xi^* = \underset{\xi}{\operatorname{argmin}} F(\xi) = \underset{\xi}{\operatorname{argmin}} \sum_{ij} e_k^T(\mathbf{x})\Omega_k e_k(\mathbf{x}) \tag{14}$$

5. Experimental verification

5.1.Software and hardware platform

In the experiment, mecanum four-wheel drive AGV car is used, and a 48v100ah lithium battery of Zhongke hongpan company is carried to provide power for the system. The bottom layer is an integrated control board with stm32f103-zet6 embedded single chip microcomputer as the main control chip, which is mainly responsible for receiving the upper layer information, controlling the movement of the car, collecting odometer information and IMU data and transmitting them to the computer. The control board integrates motor drive chip and mpu60-50 six axis motion processing component, and mpu6050 integrates three axis accelerometer and three-axis gyroscope.

The upper layer adopts industrial computer, the processor is intel core i5 5200U, 2.4 GHz, and the memory is 8g. ubuntu 16.04 system and ROS kinetic version system. Be responsible for point cloud processing and slam mapping navigation, and the upper and lower layers communicate through IIC. Odometer, IMU and lidar data are transmitted to the computer through IIC and then processed to complete the slam process. The following “Fig.2” shows the self built experimental platform.



Fig.2 Experimental platform

5.2.Comparison of drawings under outdoor environment

During the drawing process of the trolley, the linear speed of the trolley shall be fixed at 0.4 m/s, and the angular speed shall be adjusted to 0.1 rad/s. The above speed shall be applied to all the drawing processes, and there shall be no rapid acceleration and deceleration during the drawing process.

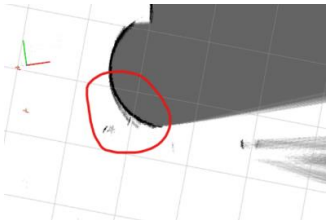

Fig 3 Original algorithm map

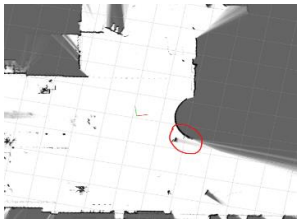

Fig 4 Map constructed by this algorithm

Connect the trolley and radar via a laptop, and control the trolley for map building. “Fig.3” above is a map built by Google's open source cartographer algorithm, it can be seen that the original

algorithm can not completely close the loop when building a large-area map, resulting in map distortion, “Fig.4” is the map built by the local to global hierarchical optimization of this article, due to the consideration of the impact of angular displacement on the map, the algorithm can effectively correct the wrong loopback.

On the premise of successful closed-loop, guide the car to five obstacles, measure the distance from the car to the fixed obstacles for ten times, and the results are shown in Tab.I.It can be seen that the accuracy of the algorithm is about 10cm in the outdoor scene.

Tab.I Statistics of drawing error

Number of tests	Obstacle1	Obstacle2	Obstacle3	Obstacle4	Obstacle5	average error
1	9.3	9.5	10.2	10.4	9.6	9.8
2	10.3	10.6	10.7	10.2	10.6	10.4
3	10.2	10.3	9.9	10.5	10.3	10.2
4	10.3	10.5	10.1	9.9	10.4	10.2
5	10.5	10.3	10.4	9.9	10.2	10.2
6	9.2	9.5	9.4	9.8	9.5	9.48
7	10.5	10.2	10.4	10.2	10.3	10.3
8	10.5	10.2	9.8	10.2	10.3	10.2
9	10.5	10.5	10.2	10.3	10.4	10.3
10	9.5	9.3	9.2	9.6	9.4	9.4

5.3.Indoor construction drawing

The experimental platform is used to map the corridor environment outside the laboratory. “Fig.5” shows the real environment of the corridor outside the laboratory, and “Fig.6” shows some renderings of the corridor environment. From the drawing effect, it can be seen that the algorithm in this paper can build a high precision global map after correcting the angle error. The map has no obvious error loop, and the drawing effect has been significantly improved.



Fig.5 Corridor environment

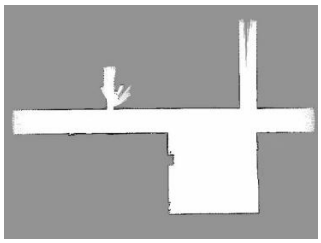

Fig.6 Laboratory corridor environment

5.4.Evaluation of public data sets

The original algorithm and the improved algorithm are tested in the public data set German museum. The quantitative analysis of the test data set is shown in the Tab.II below:

Tab.II Data set test quantitative analysis

Deutsches Museum		
	Before improvement	After improvement
Absolute translation error	1.372±1.34	0.591±0.628
Meansquare error	1.298±2.15	0.819±1.598
Absolute rotation error	2.879±4.26	1.423±2.676
Meansquare rotation error	2.362±4.62	1.734±2.047

“Table II” comprehensively evaluates the improved algorithm and the original algorithm using four kinds of errors. It is tested in the public data set German Museum, and two algorithms are used to run the data set. From the data in the table, it can be seen that the improved algorithm has a high

improvement in the quality and effect of drawing. After calculation, the absolute translation error is reduced by 48% and the absolute rotation error is reduced by 40%; The improved algorithm is helpful to improve the drawing quality and reduce the loopback error.

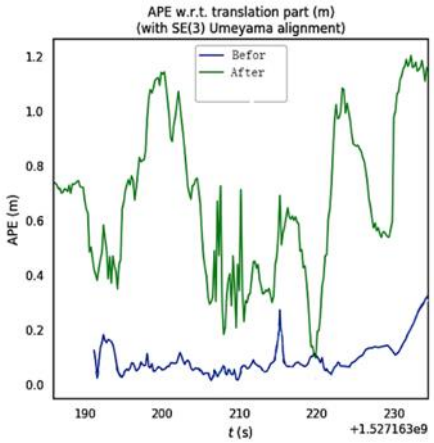

Fig.7 APE real time positioning error graph

The above "Fig.7" shows the visualization effect of this algorithm and the original algorithm when running the public data set. The algorithm is evaluated by using the ape (absolute trajectory error) evaluation index. It can be seen from the above figure that the real-time positioning error of this algorithm is much smaller than that of the original algorithm, and the map error is effectively corrected when the data fluctuates greatly. This is because the segmented loop detection is added to the front-end matching process of graph optimization, The accuracy of local map positioning is ensured, and the error function added in the segmented map optimization is corrected in the global optimization, which ensures the accuracy of global optimization and improves the accuracy of map construction.

6. Conclusion

Aiming at the problem that the open source cartographer algorithm has large cumulative errors in largescale simultaneous positioning and mapping, resulting in the global map can not be closed loop effectively, this paper proposes a hierarchical optimization algorithm based on IMU data. According to the change of IMU angular displacement, the IMU data is distributed according to the dynamic weight distribution coefficient to reduce or increase the trust value of IMU data. According to the pose information detected by the loop, the local graph is optimized and the local subgraph is constructed. Then take the radar data of the next frame as the starting point of segmentation to construct a new subgraph. According to this cycle, the global map is optimized until the map is built. After verification, this algorithm can effectively solve the problem of incomplete closed loop, and has guiding significance for large-scale slam.

References

[1] Reid M, Morgan S, Whiteside D. Match play characteristics of Grand Slam tennis: implications for training and conditioning. J Sports Sci. 2016; 34(19): 1791–1798

[2] Jaud M, Rouveure R, Faure P, et al. Method for orthorectification of terrestrial radar maps [J]. ISPRS Journal of Photogrammetry and Remote Sensing, 2014,97: 185-194.

[3] Deng Zhihong, Liu Mingyang, Fu Mengyin. An improved feature matching point extraction algorithm between visual sensor and laser ranging radar [J] optical technology, 2010, 36(1): 43-47.

[4] Ma, J, Bajracharya, M, Susca, S. (2016) Realtime pose estimation of a dynamic quadruped in GPS denied environments for 24hour operation. International Journal of Robotics Rese-arch 35(6): 631–653.

[5] Fuentes pacheco J, Ruiz ascencio J, Rendónmancha J M. Visual simultaneous localization and mapping: a survey [J]. Artificial Intelligence Review, 2015, 43(1): 55-81.

[6] Folkesson J, Christensen H. Closing t-he loop with Graphical SLAM. IEEE Trans Robotics. 2007; 23: 731-741.

[7] J.Callmer, K.Granström, J.Nieto, and F.Ramos Tree of words for visual loop closure detection in urban SLAM [C].// In Proceedings of the 2008 Australasian Conference on Robotics and Automation (ACRA), 2008: 102

[8] Newman. Probabilistic appearance based navigation and loop closing [C]// IEEE International Conference on Robotics and Automation, IEEE, 2007: 204-2-2048.

[9] Grisetti G, Kummerle R, Stachniss C, et al. A tutorial on graphbased SLAM [J]. IEEE Intelligent Transportation Systems Magazine, 2010, 2(4): 31-43

[10] D. Borrmann, J. Elseberg, K.et al. Globally consistent 3D mapping with scan matching [J]. Robotics and Autonomous Systems, 2008, 56(2): 130-142.

[11] Olson, E. April Tag: A robust and flexible visual fiducial system. In Proceedings of the IEEE International Conference on Robotics and Automation (May). IEEE, 2011, 3400-3407.